# RESERVOIR TRACER TEST AT THE NGATAMARIKI GEOTHERMAL FIELD

Etienne Buscarlet[1], Hyungsul Moon[1], Irene Wallis[1] and Jaime Quinao[1]

[1] Mighty River Power Limited, PO Box 245, Rotorua 3010, New Zealand

etienne.buscarlet@mightyriver.co.nz

**Keywords:** *Ngatamariki, Reservoir Tracer Test, Moment Analysis, Dispersion, Sorption, Modelling, Tough2*

## ABSTRACT

A reservoir tracer test was conducted at the Ngatamariki Geothermal Field following the commissioning of an 82 MW binary plant in October 2013. The objectives of the test were to assess the fluid flow pathways and potential connections between the injection and production wells. The geothermal fluid is produced from three deep wells in the centre of the field and is entirely re-injected back into four deep injection wells which are split between the northern and southern sectors of the field. In January 2014, four (4) types of Naphtalene Disulfonate tracers (1,5-NDS, 1,6-NDS, 2,6-NDS and 2,7-NDS) were introduced into the injection wells, and sampling of fluids from the production wells were carried out over a period of eighteen (18) months. Tracer returns were observed in the production wells, but with diverse responses: fast returns were observed in the south of the field (tracer breakthrough in 28 days) while returns from the northern injectors are slower (tracer breakthrough in 100 days at the earliest). The amount of tracers recovered ranged from 0.5 to 5%. Moment analysis of the tracers recovery curves, coupled with geologic context and process modelling using Tough2, have provided valuable information about the permeability pathways at Ngatamariki. The results highlight the permeability characteristics and structural features in the southern part of the resource, which correlates well with the data from the micro-seismic monitoring.

## 1. INTRODUCTION

The Ngatamariki geothermal field is located in the central part of the Taupo Volcanic Zone (TVZ), 17 km north of Taupo, New Zealand. The field was first drilled in 1984 by the New Zealand government. In 2004, the Rotokawa Joint Venture (RJV), a joint venture between Tauhara North #2 Maori Trust and Mighty River Power Limited (MRP), resumed exploration and confirmed the geothermal resource sufficient for commercial development (Boseley et al., 2010). The RJV was subsequently granted resource consent in 2010 to develop the Ngatamariki Geothermal Field with a fluid take of 60,000 t/d and 98% injection, and in October 2013 a 82 MW Ormat binary plant was commissioned.

The Ngatamariki reservoir comprises a deep, hot (260-285°C) geothermal reservoir overlain by two separate groundwater aquifers. The Ngatamariki host rocks are similar to most TVZ geothermal systems, where a volcanic-sedimentary sequence, which is dominated by rhyolitic pyroclastic and lava, volcaniclastic sediments and typically deep-buried andesitic units, overlies a metasedimentary greywacke basement. The reservoir fluid chemistry is dilute (NaCl < 0.05 molal), near-neutral (reservoir pH ~6) and high chloride (reservoir Cl~900-1000 mg/kg). Reservoir permeability is thought to be dominantly fracture-controlled (Wallis et al. 2015).

During the tracer test, geothermal fluid was produced from three deep wells in the centre of the field (in red, Figure 1) and entirely reinjected into four deep reinjection wells located on the northern and southern edges of the reservoir (in blue, Figure 1). The 2014 average daily take was 41,418 t/d and injection was split between approximately 60% to the northern injectors and 40% to southern ones (Wallis et al., 2014).

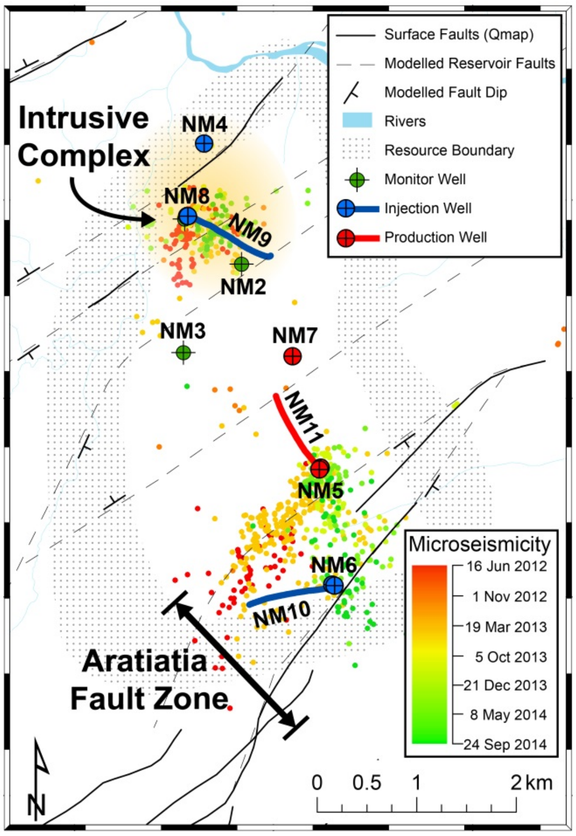


**Figure 1: Ngatamariki Geothermal Field layout during the test period. The yellow shaded zone represents the drilled area of the intrusive complex and is therefore a minimum size. Modelled reservoir faults (Wallis & Bardsley, 2015) and QMAP (2014) surface faults are included.**

In January 2014, following around 5 months of stable operation, MRP conducted a reservoir tracer test to better understand reservoir hydrogeology, fluid flow pathways and potential connections between injection and production wells. This paper presents details of the test, including its results and some interpretative outcomes.

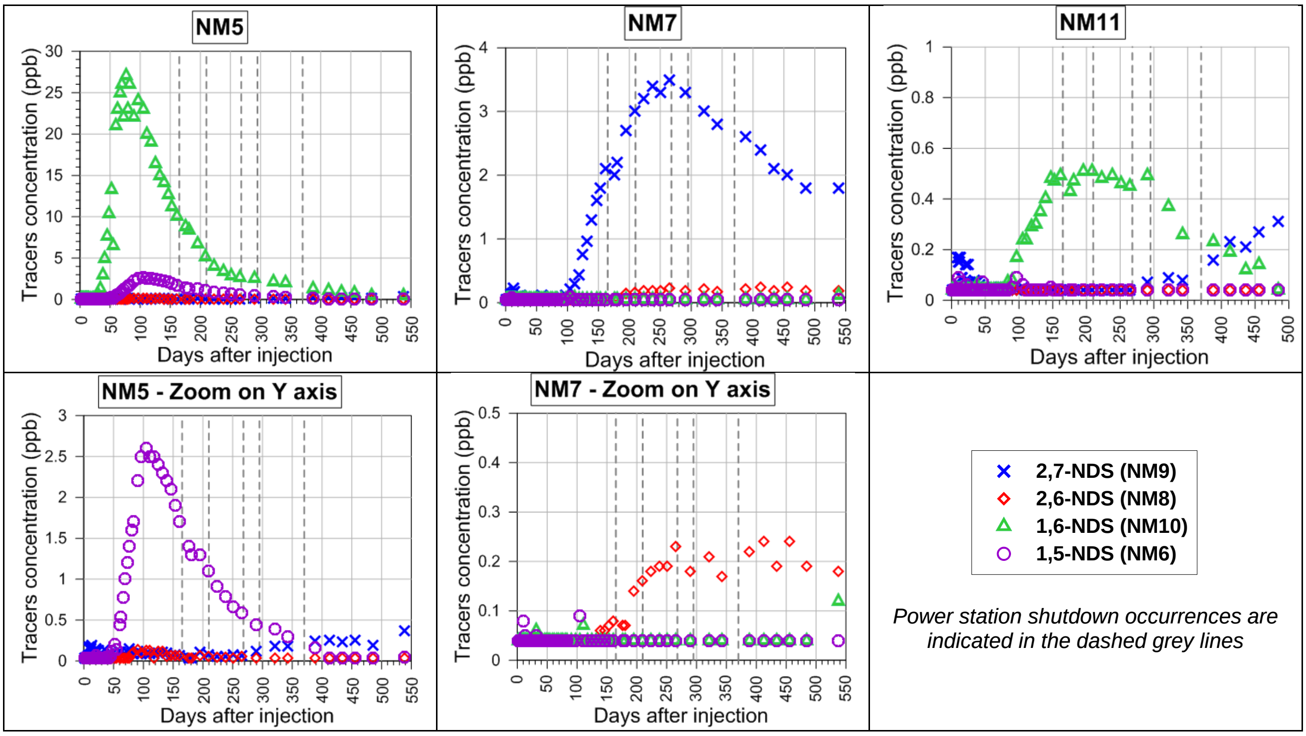


**Figure 2: Tracer returns in the Ngatamariki production wells**

**Table 1: Summary of the Ngatamariki tracer test results and moment analysis interpretation**

| Production well | Tracer recovered | First arrival time (days) | Peak concentration time (days) | Amount of tracer recovered (%) | Mean tracer velocity (m/day) | Mean tracer residence time (days) | Swept pore volume ($m^3$) | Lorentz coefficient - Lc |
|---|---|---|---|---|---|---|---|---|
| NM5 | 1,6-NDS | 27 | 76 | 10.1 | 14 | 155 | 127,620 | 0.35 |
| NM5 | 1,5-NDS | 45 | 105 | 0.3 | 11 | 172 | 31,720 | 0.26 |
| NM7 | 2,6-NDS | 139 | 413 | 0.6 | 4 | 718 | 14,380 | 0.35 |
| NM7 | 2,7-NDS | 90 | 265 | 5.6 | 4 | 480 | 863,820 | 0.32 |
| NM11 | 1,6-NDS | 83 | 200 | 0.3 | 8 | 260 | 9,300 | 0.24 |

## 2. TEST DESIGN AND TRACER INJECTION

### 2.1 Test Design

Reservoir tracer tests can provide powerful insights into geothermal reservoir characteristics. Polyaromatic sulfonates compounds have proven to be suitable chemical tracers at geothermal conditions (Rose et al., 2001, 2002). Following MRP's experience with these groups of compounds in reservoir tracer testing at Rotokawa (Winick et al., 2015, Addison et al, 2015), the stability of selected polyaromatic sulfonates was investigated in a laboratory study (Mountain and Winick, 2012). Based on that study, four naphthalene disulfonic acids salts (NDS) were chosen for Ngatamariki (namely the 1,5-, 1,6-, 2,6-, and 2,7-NDS), because the experiment showed they would be stable at 280°C, the inferred reservoir temperature.

### 2.2 Tracer Injection

The dosing rate was determined by assuming the magnitude of returns under operating conditions and estimating the minimum amount necessary to be detectable. The dosing method aims at minimizing the amount of tracer used to reduce the impact on background reservoir concentration for future tests. On January 7$^{th}$ and 8$^{th}$ 2014, 200 kg of 2,6-NDS, 400 kg of 2,7-NDS, 250 kg of 1,6-NDS and 400 kg of 1,5-NDS were injected into NM8, NM9, NM10 and NM6 respectively. Each NDS isomer was pre-mixed with around 3000 L of river water, and the slurry was injected at the injector wellhead through a 2" side-valve, followed by a flush of additional 2000 L of river water. Injection was performed with an 18 bar-rated pump, within the shortest time possible to ensure an almost instantaneous tracer flux in the reservoir.

### 2.3 Sampling and Analysis

Sampling began prior to the injection of the tracers to assess the background reservoir concentration of these chemicals. Samples consisted of 100 ml fluid collected using stainless-steel cooling coils, and analyzed by high performance liquid chromatography (HPLC) using fluorescence detection at the New Zealand Geothermal Analytical Laboratory (NZGAL), GNS Science Wairakei. Detection limits were 0.04 parts per billion (ppb). No NDS were detectable in the reservoir prior to the tracer test. Sampling and samples analyses were carried out for 18 months after tracer injection.

## 3. TEST RESULTS

Within 6 months all the injected tracers were detected at the production wells. Figure 2 and the first four columns of Table 1 show the raw tracer breakthrough curves and their characteristics. Mean tracer velocity is estimated by averaging the mean velocity of all recovery curve data points. Power station shutdowns for partial or full maintenance cause hiatuses in production/injection which variably offset the recovery curves, but with negligible impacts on analysis and interpretation of the recovery curves.

Analyses of the recovery curves suggest the following characteristics for the Ngatamariki reservoir:

- The shape of the return curve (similar to a log-normal distribution) and the amount of 1,6-NDS recovered in NM5 (more than 10%) suggest a direct channel connecting NM10 and NM5. This connection likely relates to a north-east microseismic lineament which is spatially coincident, and is further investigated in section 4.3.
- The second highest recovery rate is seen in NM7, where returns from NM9 are more distributed over time, indicating a longer, more complex return pathway. Amount recovered is higher than 5%.
- Tracer returns suggest that connections from NM6 to NM5, NM10 to NM11 and NM8 are distributed, similar to the NM9 to NM7 result, and recovered amount is minor (<1%).
- Small amounts of 2,7-NDS were recovered in NM5 and NM11 toward the end of the sampling period. These returns are most likely tracers recycling, based on the timing of their occurrences. NM7 being the biggest producer in the field (an average 950 t/h for 2014, Wallis et al., 2014), 2,7-NDS is effectively reinjected at the highest rate in all the reinjection wells. These returns are believed to come from NM10 and NM6.

Direct comparisons between the four NDS result sets should be made with caution as the amount of tracers injected in each wells was not identical. However, arrival and peak concentration times immediately suggest that connection between injection and production is faster in the south than the north, in particular the presence of a direct channel connecting NM10 and NM5. Yet tracer results generally reveal a high degree of connectivity between injection and production, consistent with the Ngatamariki conceptual model (Boseley et al. 2010, Clearwater et al. 2012).

Overall, tracer recovery rates during the 2014 test were relatively small. It is similar to tracer return rates encountered at the Rotokawa field, located a few kilometers to the south (from <1% to ~7%, Addison et al., 2015).

## 4. INTERPRETATION

### 4.1 Moment Analysis

The moment analysis approach was applied to the tracer data (Shook and Forsmann, 2005) to infer reservoir properties. Moment analysis determines tracer residence times on the basis that tracer breakthrough curves usually closely match a probability distribution function and, as such, statistical properties can be assessed. Those residence times can be used to infer the fracture volume swept by the tracer and flow geometry parameters. Valuable applications of this method have been recently presented for the 2013 Rotokawa Geothermal Field tracer test (Winick et al., 2015) and the 2012/2013 tests at Habanero Engineered Geothermal System (Ayling et al., 2015).

Moment analysis assumes that the injection/production scheme is in steady-state, and the tracer is ideal and conservative.

Based on the inferred thermal stability of the tracers used (discussed in Section 2), it is also assumed that no thermal decay is occurring and therefore no correction is needed. An apparent age distribution function is computed and corrected for tracer recycling effects (the produced tracers being continuously reinjected in the reservoir). The breakthrough curve is extrapolated using an exponential function fitted to the tail of the curve, as illustrated in Figure 3.

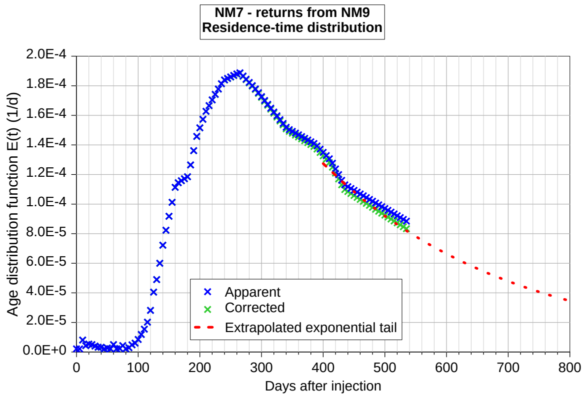


**Figure 3: Apparent and corrected age distribution function and exponential extrapolation of the tail for the 2,7-NDS tracer return in NM7.**

The three last columns of Table 1 present the results of the moment analysis applied to the Ngatamariki tracer data:

- Tracers' residence times in the reservoir range from 150 to 720 days. They are shorter in the south, where injection appears to reach the Pad B production area in less than a year, whereas they are longer in the north, with returns within one to two years.
- Total fracture volume swept by tracer is significantly higher from NM9 to NM7 than along the rest of the flow pathways. If we assume that 1% of the rock mass is fracture—a reasonable assumption based on both model and in-well observations— a rock mass dimensioned ~1000 m x 300 m x 300 m (length, width, depth) could have been visited by the tracer along its journey from NM9 to NM7, with 1000 m being approximately the distance between injection and production wells. Similarly, the swept pore volume from NM10 to NM5 could correspond to ~1000 m x 100 m x 150 m (length, width, depth).

The moment analysis method also provides means to estimate the relationship between the flow capacity (F - the normalized cumulative tracer recovery) and the storage capacity (Φ) of the formation (–defined as the time-weighted swept pore volume at time t)—a process herein referred to as the F- Φ approach. As shown in Figure 4, the F-Φ cross-plot is a diagnostic tool which indicates what fraction of the pore volume contributes to which fraction of the flow—essentially an estimate of how channelized flow is.

The F-Φ approach for two well pairs from Ngatamariki are presented in Figure 4 and compared to two Rotokawa pairs and a pair from the Habanero-EGS. The F-Φ approach has yielded results which are consistent with the resource conceptual models. Figure 4 shows that overall the reservoir fracture network at Ngatamariki appears to be heterogeneous, since half of the flow produced is travelling through little more than 25% of the void space determined in the moment analysis. However, despite the NM10-NM5 return curve shape indicating channelized flow and NM9-NM7 indicating a more distributed network, both well pairs have similar F-Φ results. This may indicate a limitation of the F-Φ approach or that there is insufficient difference in the connection between these two pairs to be detected by this analysis.

For context, the portion of reservoir between the well pair tested during 2013 at Rotokawa (Winick et al., 2015) showed more homogeneity than any of the other wells pairs presented herein, and was thought to reflect a relatively evenly distributed set of fractures. The high degree of heterogeneity in the Habanero well pair is an expected attribute for an EGS system. Finally, the 2006 RK17-RK18 test supports the hypothesis of a highly channelized flow, which was also indicated by the tracer return curve shape, fast first arrival time (8 days) and the well positions along the structural grain (Addison et al, 2015).

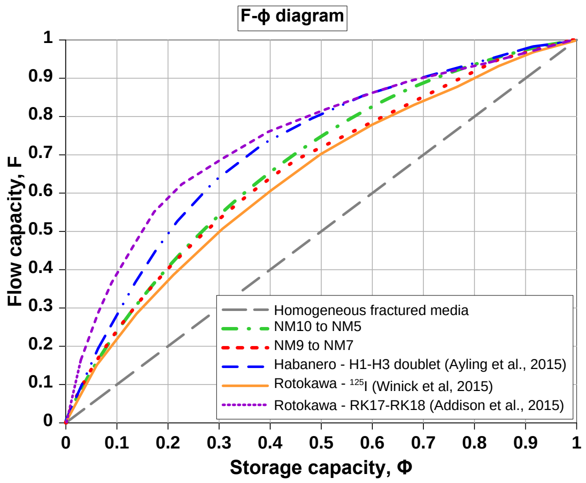


**Figure 4: F-Φ plot for Ngatamariki wells and selected fields**

The Lorentz coefficient ($L_C$) can be determined from the F-Φ cross-plot and is a measure of the heterogeneity of the formation. $L_C$ ranges from 0 (homogeneous) to 1 (most heterogeneous). $L_C$ values for Ngatamariki wells pairs (Table 1) show that flow pathways from the southern injectors to production are more uniform than flow pathways from the northern injectors. The $L_C$ values therefore suggest a more complex permeability structure in the north of the field, which is likely related to the presence of a large intrusive body at depth and into which the northern injectors are terminated. The permeability pathway complexity would stem from the interplay between the intrusive—its low permeability interior and surrounding damage zones, as well as impact of relic alteration on adjacent host-rock mechanical properties—and the wider fracture network of the reservoir.

### 4.2 Groundwater Analogy

Because Ngatamariki is a single phase liquid reservoir and some recovery curves are strikingly similar to what is commonly encountered in a groundwater context, it is valuable to apply analytical solutions widely used in this domain to understand some aspects of the tracer test results.

There are some limitations as the solutions applied in groundwater systems are isothermal, and parameters such as the hydraulic conductivity are not straightforwardly comparable to a geothermal permeability. However, this approach provides (i) a conceptual framework which emphasizes the mechanism of the tracer movement within the reservoir and (ii) a semi-quantitative description of transport behaviours usually disregarded in geothermal numerical models, such as the kinematic dispersion of the tracers within the reservoir (mixing caused by the heterogeneities of the flow velocities in the formation) and sorption of the tracers to the reservoir rocks. The breakthrough curves analytical interpretation was achieved using TRAC: a computer tool for tracer-test interpretation developed by BRGM, the French Geological Survey (Gutierrez et al., 2013). Two examples of this analytical approach are presented in Figure 5:

- The breakthrough curve of tracer from NM10 to NM5 can be closely matched using an analytical solution corresponding to a brief injection of mass (Dirac injection) in a 1-D infinite medium where a uniform flow occurs with a constant dispersion. In effect, the kinematic dispersion spatially spreads and attenuates the tracer plume concentration in the reservoir. The dispersion is characterized by a dispersivity coefficient (α) which is a distance, and an intrinsic property of the formation; it quantifies the heterogeneities in the advection process, and also depends on the scale of observation. In this example the dispersion coefficient is about one tenth of the distance between NM10 and NM5, which is a typical range for α. The cross-sectional area *A*=820 $m^2$ provides a quantitative estimate of the fracture dimension connecting NM10 to NM5. This mono-dimensional approach is similar to the interpretation method proposed in the *TRINV* software (Axelsson et al., 2005).
- Returns from NM9 to NM7 are matched with a solution corresponding to a Dirac mass injection in a 2-D infinite medium with constant dispersivity (both transversal and longitudinal). This solution also considers a delay coefficient (R) to account for sorption of the tracers to the reservoir rocks, resulting in attenuation and retardation of the tracer signal. This coefficient uses the $K_d$ approach (linear sorption isotherm), which has many limitations but may be applicable for organic compounds such as the naphtalene disulfonates. The good agreement of the analytical solution with the observation indicates that such phenomenon is likely occurring in the reservoir. The longitudinal dispersivity coefficient is relatively high compared to the distance between NM9 and NM7 and is higher than the southern area despite the shorter distance between NM9 and NM7. This value for dispersivity emphasizes again the permeability heterogeneities in the northern area. The transversal dispersivity is very small, and on the high end of the typical $\frac{\alpha_L}{\alpha_T}$ ratio encountered in field experiments (commonly 10 to 100). This small value is likely due to the fracture-controlled nature of the permeability in the reservoir, and dispersion perpendicular to the flow is in fact close to diffusion (mixing due to concentration gradients).

| *Observed versus computed breakthrough curves* | *Conceptual diagram and analytical solution (Adapted from Gutierrez et al., 2013)* | *Selected fitted parameters* |
|---|---|---|
| 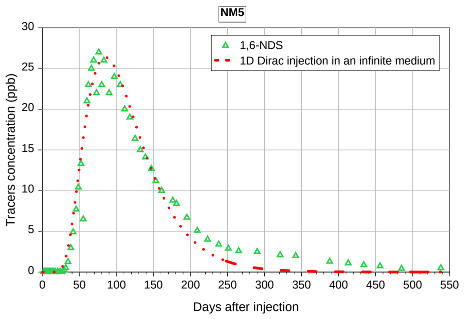 | Dirac injection in a 1-D uniform flow, infinite medium 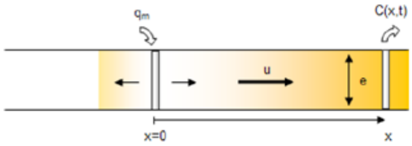 $C(x,t) = \frac{M_0}{A\omega\sqrt{4\pi D_L t}} exp\left[-\frac{(x-ut)^2}{4D_L t}\right]$ | $\omega = 0.7$<br>$v = 11$ m/d<br>$A = 820$ m$^2$<br>$\alpha_L$=150 m |
| 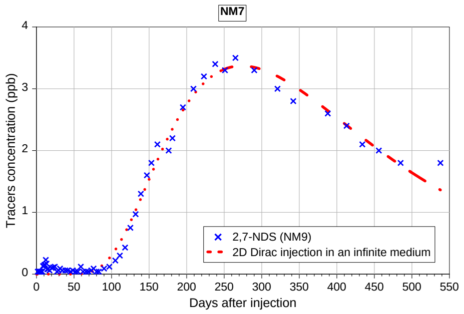 | Dirac injection in a 2-D uniform flow, infinite medium 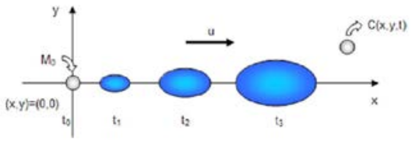 $C(x,y,t) = \frac{M_0}{4\pi e\omega t\sqrt{D_L D_T}} exp\left[-\frac{(x-\frac{u}{R}t)^2}{4\frac{D_L}{R}t} - \frac{y^2}{4\frac{D_T}{R}t}\right]$ | $\omega = 0.7$<br>$v = 4$ m/d<br>$e = 130$ m<br>$\alpha_L$=190 m<br>$\alpha_T$=0.05 m<br>$R$=1.5 |

**Figure 5: Observed and modeled breakthrough curves using analytical solutions**

**Symbols and notations:** $C$ (kg/m$^3$) = concentration of tracer at point ($x$,$y$) and time ($t$); $M_0$ (kg) = mass of injected tracer; $e$ (m) = aquifer thickness; $A$ (m$^2$) = cross-section area of the aquifer transverse to the flow; $\alpha_L$, $\alpha_T$ (m) = longitudinal/transversal dispersivity coefficient; $\omega$ = effective porosity (0< $\omega$ <1); $u$ (m/s)= pore velocity; $v$ (m/s) = Darcy's velocity ($v$=$u$ x $\omega$); $D_L$,$D_T$ (m$^2$/s) = longitudinal/transversal dispersion ($D_L$= $\alpha_L$ x $u$; $D_T$= $\alpha_T$ x $u$); $\rho$ (kg/m$^3$) = aquifer density (kg/m$^3$); $R$ = delay coefficient ($R = \omega + \rho K_d$); $K_d$ (m$^3$/kg) = distribution coefficient (Linear sorption isotherm coefficient).

Finally, the value of the aquifer thickness ($e$ = 130m) is small compared to the thickness of the reservoir based on inference testing and indicates that the flow may be confined to preferential pathways.

### 4.3 Reservoir Structure and Microseismicity Trends

Ngatamariki geology comprises a faulted stack of volcanic, dominantly rhyolitic and andesitic, and volcaniclastic/sedimentary deposits which overlie a metasedimentary basement and, in the north, contain a dioritic to tonalitic intrusive complex. Chambefort et al. (2014) has a detailed description of stratigraphy while Wallis and Bardsley (2015) discusses likely extents of reservoir rocks and structures. Information on alteration mineralogy, with particular reference to the intrusive, can be found in Chambefort et al. (2015).

The key feature influencing the southern Ngatamariki hydrology, particularly the connection between NM10 and NM5, is the Aratiatia Fault Zone (AFZ): an active fault zone (QMAP 2014) along which microseismicity has been migrating since losses were encountered while drilling the NM10 production section (Figure 1). NM6, which also occurs within the AFZ, is completed off-strike relative to NM5 and therefore is not expected to have the degree of direct connection observed in NM10. Tracer returns (Figure 2) are consistent with this observation. In contrast to the simple structural connections of the south, the northern geology and hydrology is influenced by a complex mix of faulting and the large intrusive complex present below ~1500 mVD. The injection well NM8 (a low permeability injector) is completed into the heart of the intrusive complex. While also being completed into the intrusive, NM9 (which has higher permeability than NM8) appears to intersect a recently active structure above the intrusive complex and a deep zone of densely fractured rock thought to be an intrusive-related damage zone. In contrast with the south, microseismicity around NM8 and NM9 is more clustered and shows no clear migration with time toward production (Figure 1). Taken together, geologic observations support the interpretation that there is a relatively more complex connection between injection and production from northern injectors than there is from the south.

### 4.4 Tough2 modelling approach

Tough2 modelling has been applied with successful outcomes for the reservoir understanding and commercial decisions at Ngatamariki (Clearwater et al. 2012, Moon et al., 2014). Process modelling is a powerful approach to refine the reservoir understanding and test hypotheses, and has been applied to the tracer tests results. The modelling is conducted using EOS1, designating the tracer as secondary water ("water 2").

In this approach, only a part of the southern area of the full field model (Clearwater et al., 2012) is utilised and highly discretized. The resulting three-dimensional model is made of 9072 blocks and covers an area of 1.75 km by 2.925 km, with an elevation of -500 m to -3200 mRL. The following parameters were used in the model setup:

- The reservoir rock properties are the same as the full field model rock properties: it is a dual-porosity model, treating matrix and fracture separately. The fracture permeability and fracture volume of selected blocks between NM10 and NM5 were modified to reflect the role of the AFZ and to match the observed tracer breakthrough curve shape in NM5;

- The initial reservoir temperature is set uniformly at 280ºC and initial reservoir pressure is calculated by Tough2 based on this temperature;
- There are no boundary conditions. This simplification has little consequences on the modeled results in regard to the process and timeframe considered.

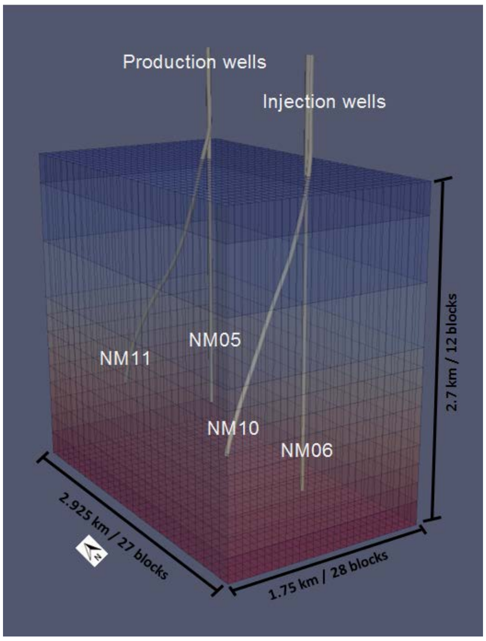


**Figure 6: Grid system of Ngatamariki tracer model**

The process model is therefore a completely closed system which is run for about 220 days. At t=0, actual production and injection flow rates are implemented in NM5/NM10 and NM6/NM10 respectively; while a flux of water 2 is injected into NM6 in a first run and into NM10 in a second run, in volumes and at rates equivalent to the field test conditions (tracers were injected within ~20 minutes).

The aim of process modeling was to match (i) the arrival time of the tracers and (ii) the peak concentration time of the tracers. A major limitation of this modelling exercise, however, lies in the fact that it is not appropriate to compare observed and modelled amount of tracers. As mentioned earlier, hydrodynamic dispersion and chemical processes (thermal decay, sorption) are usually not taken into account in Tough2, and the process model is restricted to a very small portion of the reservoir. The modelled tracer behaviour is therefore excessively conservative, and subsequently the modelled mass of tracer recovered would not be expected to match the real-world recovered concentration.

Figure 7 and Figure 8 present the modelling results for the tracers' breakthrough curves in NM5. The amount of modelled tracers ("water 2 fraction" on the right hand side of the plots) is arbitrarily attributed to a tracer concentration for plotting purpose (e.g. for NM10, a water 2 fraction of $10^{-5}$ corresponds to ~15 ppb, whereas it corresponds to ~2.5 ppb for NM5). As mentioned above, matching the arrival time is the main goal of the modelling exercise, and ultimately does not depend on the amount of tracers injected. This latter aspect of the modelling has been ignored in the analysis.

Fluid velocity is the main control on the tracer arrival and peak times to the production. The Darcy's law relates the volume flux (or Darcy velocity) to the permeability through the following empirical relationship:

$$q = \frac{-k}{\mu} \nabla p$$

where q is the mass flux (discharge per unit area, m/s), $\nabla p$ is the pressure gradient (Pa/m), $\mu$ the fluid viscosity (Pa.s) and $k$ the permeability ($m_2$). The fluid velocity is in turn related to the Darcy velocity through the following equation:

$$v = \frac{q}{\emptyset}$$

where $v$ is the fluid velocity (m/s) and $\emptyset$ the porosity. In Tough2 with dual porosity, the fracture porosity is equal to the fracture volume. The calibration process was therefore conducted focussing mainly on fracture permeability and fracture volume.

To match the tracer's arrival and peak times in NM5, it was necessary to consider an area between NM10 and NM5 with a fracture's permeability more than 20 times higher than the surrounding reservoir. Best matches between observed and modelled recovery curves are obtained when the fractures in the fault zone have a permeability of 1 to 3 Darcy, while the fracture volume is 0.8%. This latter value is in good agreement of in-well measurements of fracture volume (Wallis et al., 2015).

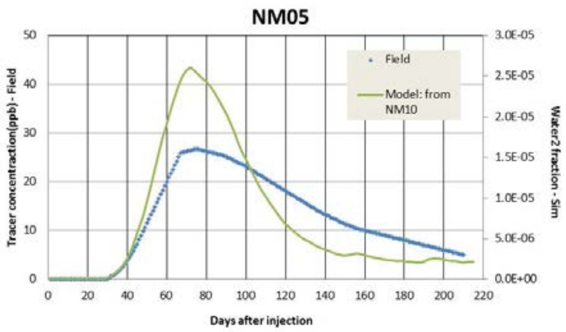


**Figure 7: Modeled Water 2 fraction in NM5 (from NM10)**

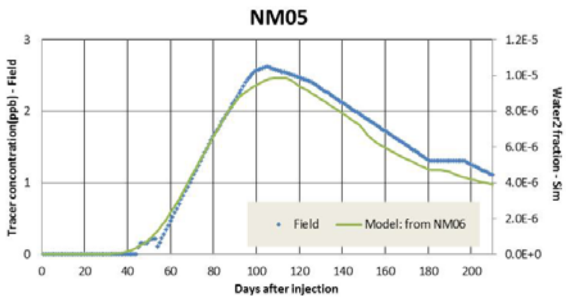


**Figure 8: Modeled Water 2 fraction in NM5 (from NM6)**

The process model emphasizes the role of the AFZ in tracer test returns between NM10 and NM5. The tracer modeling also provides a range of reasonable values for rock properties to be used in the full field model.

### 5. RESERVOIR MANAGEMENT IMPLICATION

The reservoir tracer test results inform the reservoir management through a better understanding of inter-well connectivity and the risks associated with unfavourable connections.

The tracer information showing direct flow channelling from NM10 to NM5 resulted in reduced injection into NM10. At present, NM10 is shut-in and only used intermittently. The balance of injection required has been shifted to the other injection wells that had a more distributed tracer return curve.

In addition to changes to the injection system, the reservoir surveillance program was also adjusted based on the tracer results. Production monitoring and downhole temperature surveys were augmented to detect early signs of thermal breakthrough.

The tracer return curves and the modelled permeability characteristics are used for further studies leading to improved resource conceptual models and numerical models.

The adaptive reservoir management approach used in Ngatamariki ensured that the tracer test results influence the reservoir management strategy while managing the requirements of an operating field. At present, injection is successfully redistributed, NM10 is only used intermittently and future injection well locations consider the tracer information. Production wells NM5 and NM7 show no substantial changes in enthalpy. A new production well (NM12) was drilled west of the NM5 area. It was brought online in 2014, redistributing the production load and reducing the risk of thermal breakthrough.

## 6. CONCLUSION

The Ngatamariki reservoir tracer test has provided useful insights into the nature of subsurface permeability and the connections between injection and production wells, information which has been applied to the management of key reservoir risks. Due to the well-connected permeability at Ngatamariki, all the tracers were recovered in one or more production wells. Test interpretation has been greatly facilitated by the fact that the recovery curves were close to ideal cases, something which is far from typical in geothermal reservoirs.

Several tools have been used in the interpretation of the tracer test, each providing different kind of information. The temporal moment analysis provided the tracers mean tracer residence time and an understanding of the heterogeneities in the reservoir. Analytical solutions commonly used in fresh groundwater systems identify tracer transport behaviour such as dispersion and sorption, which are likely to occur in the reservoir. Process modelling highlighted the importance of an active fault zone in the fastest tracer return result, while also refining fracture volume and permeability.

The overall low rates of recovery (from <0.1% to 10%) and the process modelling results indicate that the NDS compounds used in the Ngatamariki reservoir may not be totally stable. Although laboratory experiments proved that no thermal decay was occurring up to 280ºC-300ºC, tracer breakdown is likely taking place under longer residence times. It is one area of investigation to re-analyse the samples for breakdown products such 1-NSA and 2-NSA.


## ACKNOWLEDGEMENTS

The authors wish to thank Western Energy Services, the New Zealand Geothermal Analytical Laboratory (NZGAL) at GNS Science and MB Century which greatly contributed to the test achievement. Jonathon Clearwater and Farrell Siega are gratefully thanked for their thorough review and constructive comments.


## REFERENCES


Addison, S.J., Winick, J.A., Mountain, B.W. and Siega, F.L., 2015 Rotokawa Tracer Test History *Proc. 37th New Zealand Geothermal Workshop, 2015, Taupo, New Zealand*

Ayling, B.F., Hogarth, R.A. and Rose, P.E., 2015, Tracer Testing at the Habanero EGS Site, Central Australia, *Proceedings of the World Geothermal Congress, Melbourne, Australia, 2015*

Axelsson G., Bjornsson G. and Montalvo F., 2005, Quantitative Interpretation of Tracer Test Data, *Proceedings of the World Geothermal Congress, Antalya, Turkey, 2005*

Boseley C., Cumming W., Urzua-Monsalve L., Powell T. and Grant M., 2010, A Resource Conceptual Model for the Ngatamariki Geothermal Field Based on Recent Exploaration Well Drilling and 3D MT Resistivity Imaging, *Proceedings of the World Geothermal Congress, Bali, Indonesia, 2010*

Chambefort, I., Buscarlet, E., Wallis, I.C., Sewell, S. and Wilmarth, M., 2015, A Review of the Ngatamariki Geothermal Field, New Zealand. *Geothermics (2015),* http://dx.doi.org/10.1016/j.geothermics.2015.07.011

Chambefort, I., B. Lewis, et al. Wilson, C. J. N., Rae, A. J. Coutts, C, Bignall, G. and Ireland, T. R., 2014. Stratigraphy and structure of the Ngatamariki geothermal system from new zircon U-Pb geochronology: Implications for Taupo Volcanic Zone evolution. *Journal of Volcanology and Geothermal Research 274: 51-70.*

Clearwater J, Burnell J. and Azwar L., 2012, Modelling the Ngatamariki Geothermal System, *Proceedings of the 37th Workshop on Geothermal Reservoir Engineering, Stanford,* SGP-TR-194, 2012

Gutierrez A., Klinka T., Thiéry D., Buscarlet E., Binet S., Jozja N., Défarge C., Leclerc B., Fécamp C., Ahumada Y. and Elsass J., 2013, TRAC, a collaborative computer tool for tracer-test interpretation, *TRACER 6 - The 6th International Conference on Tracers and Tracing Methods,* EPJ Web of Conferences 50, 03002 (2013) http://dx.doi.org/10.1051/epjconf/20135003002

Moon, H., Clearwater, J., Franz, P., Wallis, I. and Azwar, L., 2014. Sensitivity analysis, parameter estimation and uncertainty propagation in a numerical model of the Ngatamariki Geothermal Field, New Zealand. *Proceedings, Thirty-Ninth Workshop on Geothermal Reservoir Engineering, Stanford University, CA.*

Mountain, B. and Winick, J., 2012, The Thermal Stability of the Naphtalene Sulfonic and Naphatalene Disulfonic Acids under Geothermal Conditions: Experimental results and a Field-Base Example, *Proc. New Zealand Geothermal Workshop, 2012, Auckland, New Zealand*

QMAP Heron, D.W. (custodian), 2014. *Geological Map of New Zealand 1:250 000.* GNS Geological Map 1. Lower Hut, New Zealand.

Rose, P.E., Benoit, D. and Kilbourn, P: The application of the polyaromatic sulfonates as tracers in geothermal reservoirs. *Geothermics 30, 617 - 640 (2001).*

Rose, P.E., Benoit, D. and Lee, S.G., Tandia, B., Kilbourn, P: Testing the naphthalene sulfonates as geothermal tracers at Dixie Valley, Ohaaki and Awibengkok. *Proc. 25th Workshop Geothermal Reservoir Engineering*, SGP-TR-165 (2002)

Shook, G.M. and Forsmann, J.H., 2005, Tracer interpretation using temporal moments on a spreadsheet, *Idaho National Laboratory Report,* INL/EXT-05-00400

Wallis I., Azwar L., Moon H., Clearwater J., Quinao J. and Barnes M., 2015, Perspectives on permeability: Definitions of permeability with examples from the Ngatamariki Geothermal System, *Proc. 37th New Zealand Geothermal Workshop, 2015, Taupo, New Zealand*

Wallis I, Buscarlet E. and Quinao J., 2014, Ngatamariki Annual Report 1 January 2014 – 31 December 2014, *Waikato Regional Council*, New Zealand

Winick, J., Siega, F., Addison, S., Richardson, I., Mountain and B., Barry, B., 2015, Coupled Iodine-125 and 2-NSA Reservoir Tracer Testing at the Rotokawa Geothermal Field, New Zealand, *Proceedings of the World Geothermal Congress, Melbourne, Australia, 2015*